

Time evolution of photon propagation in scattering and absorbing media: the Dynamic Radiative Transfer System.

A. Georgakopoulos^{*a}, K. Politopoulos^a and E. Georgiou^b.

^a*Biomedical Optics & Applied Biophysics Laboratory, School of Electrical and Computer Engineering, National Technical University of Athens, Heroon Polytechniou 9, 15780 Athens, Greece*

^b*Department of Electrical Engineering, Technological Educational Institute of Crete, 71004 Stavromenos, Heraklion, Greece*

**Corresponding Author: Tel: +30-2107723048, Fax: +30-2107723894*

E-mail address: tassosgeo@central.ntua.gr (A. Georgakopoulos)

Abstract

A new dynamic-system approach to the problem of radiative transfer inside scattering and absorbing media is presented, directly based on first-hand physical principles. This method, the Dynamic Radiative Transfer System (DRTS), calculates accurately the time evolution of photon propagation in media of complex structure and shape. DRTS employs a dynamical system formality using a global sparse matrix which characterizes the physical, optical and geometrical properties of the material volume of interest. The new system state vector is generated by the above time-independent matrix, using simple matrix-vector multiplication – addition for each subsequent time step. DRTS simulation results are presented for 3-D light propagation in different optical media, demonstrating greatly reduced computational cost and resource requirements compared to other methods. Flexibility of the method allows the integration of time-dependent sources, boundary conditions, different media and several optical phenomena like reflection and refraction in a unified and consistent way.

Keywords: Radiative Transfer, Dynamic System, Multiple Scattering, Turbid media, Diffusion.

1. Introduction

Radiative transfer equation describes the statistical behavior of photon travel through scattering and absorbing media. This equation has been used in many scientific areas such as astrophysics[1-3], oceanography, high energy physics (neutrino transport)[4], thermal transfer[5-7], image processing and, in recent years, bio-sciences[8-11]. Many different solutions or approximations have been proposed[12], such as Monte Carlo[13, 14], Diffusion Approximation, several estimations using different basis functions[4, 6, 15-17], Finite-Element-like methods (FEM)[1, 5, 7] and combinations of them[8, 10, 18, 19]. In a very simple case a solution has been found based on a “moving” unity partition of normal distribution, decreasing over time by an exponential factor according to the absorption parameter. Because of mathematical difficulties[20-23], procedures based on Mode Carlo (MC) methods are believed to be the best practice, since calculations are going down to physical processes. Parallel array processors have been used[24, 25] to handle the huge amount of calculations required by this type of methods. Usually in standard MC techniques only space partition is implemented, so there is a lack of “time information” and these are not suitable to describe transient phenomena. Specifically, since only spatial information is given, there is no practical way to convolve the results with any specific pulsed-shaped source. In time-dependent MC[26, 27], as the method generally requires computational effort proportional to the dynamic range of the expected values – in our cases on the order of 10^{20} – the computational requirements explode especially in systems with dense partitioning in space, direction and time. These MC shortcomings are particularly evident in cases involving ultra-short light pulses.

Diffusion approximation connects the directed flow with undirected flow by a constant that simplifies the mathematical problem and turns it to an elliptical partial differential equation. But this is not physically true near sources or near boundaries. Another approach, use of spherical harmonics [4, 6, 20, 23], does not lead to an applicable solution because of the symmetry of base functions that makes almost impossible to represent a direct flow. Complicated structures such as the human body lead to discretization or to partitioning Euclidean space and create mesh structures. Mathematical approximations based on finite element methods have been proposed by many authors [1, 5, 7, 28]. These methods however do not preserve the positivity of intensity and produce potential instabilities because of the mathematical type of the RTE model. A combination of FEM with Diffusion approximation reduces the instability but does not fully resolve the problem [8, 18, 19].

The above refer to steady-state problem behavior. Time-dependency of photon transport has been attempted to be solved by Fourier transform [8, 21], “Time-dependent Monte-Carlo” or other methods[29-33]. This can be an approximate solution only when source changes are slow enough compared to effects produced by scattering rates. Under these circumstances, intensity will represent the mean-time value under the effect of power source changes. But when changes are fast, frequencies of the source will be convolved with the frequencies of the system, a fact that makes computations impractical for very short time – scale phenomena, due to the range of frequencies involved, which tend to infinity. Recent developments in medical diagnostics, however, using fs laser pulses, for e.g. for internal tumor imaging, will require accurate solutions of the radiation propagation problem in absorptive-diffusive media in very short time scales. In such cases DTRS is quite capable to deliver accurate results, where other methods are questionable.

The drawback of any mathematical method used emanates from the behavior of radiative transfer equation [22, 34, 35]. Let’s assume for a moment that absorption coefficient is zero. Then the solution of the equation will be *any* intensity that has a constant value.

$$\frac{1}{c} \frac{\partial I(\mathbf{x}, \mathbf{s}, t)}{\partial t} + \frac{\partial I(\mathbf{x}, \mathbf{s}, t)}{\partial s} - (\mu_a + \mu_s)I(\mathbf{x}, \mathbf{s}, t) + \mu_s \iint I(\mathbf{x}, \mathbf{s}', t)g(\mathbf{s}, \mathbf{s}')ds' = 0$$

$$\xrightarrow{\lim \mu_a \rightarrow 0} I(\mathbf{x}, \mathbf{s}, t) = \text{constant} \quad (1)$$

Clearly, a physical model like RTE which attempts valid predictions vs time ought to be causal. This means that there should be no output in the absence of any input, a fact that in the above example is violated. This example should not be taken as just an extreme situation, but rather as a common occurrence especially in highly-scattering media, as biological tissue. Specifically, in cases such human body tissue, scattering coefficient is hundreds of times higher than absorption coefficient. This means that any approximation algorithm constructed under the RTE will have the tendency to equalize the intensity, especially in thick volumes where the applied boundary conditions have small effect. Another serious physical problem is that RTE does not include energy transfer bounded by the speed of light. This RTE limitation will be evident in the discussion section below.

To overcome all these problems originating from RTE, a new method is described in this paper, based on the physical photon-matter interaction in a consistent treatment. This method, the Dynamic Radiative Transfer System (DRTS), computes the time evolution of photon distribution inside scattering absorbing media by the construction of a probabilistic dynamic system. This is especially useful in bio-engineering for e.g. solving the Optical Tomography “forward problem”[36] using pulsed excitation.

In comparison, RTE provides a conceptual framework for a simple description of the physical phenomenon, while, especially for the purpose of instrument design, the new DRTS method provides a tool that allows an accurate measurement system implementation. Therefore DRTS can be viewed as an improved and generalized solution method, accurately treating time effects in both short and long time scale, which avoids the inconsistencies and drawbacks of the RTE model.

In the next section the physical phenomenon will be expressed as a dynamical system and the computation of the system matrix elements will be detailed. Time evolution of the photon propagation can afterwards be computed by the simplest linear algebra operations (array-vector multiplication and vector additions). Then, the algorithm based on the theoretical analysis is constructed and simulation results are shown for some simple isotropic media with different optical properties. In the last section, a thorough comparative analysis of DRTS vs. the other methods will be detailed.

2. Modeling Photon transmission through scattering and absorbing media

On the road to create the Dynamic Radiative Transfer System (DRTS) we have to keep in mind the numerical calculation procedure and subsequent application in computers. To this purpose, creating a system of differential equation is not the best way of calculation, especially when applied in complicated structures. Since the aim is the calculations; in real world where complex volumes are present, the route lies in discretization and approximation.

To be successful we need to partition the time, the travelling direction and the Euclidean space. For calculation purposes time partitioned in small equally spaced steps Δt . According to the physical process photons propagating inside the media will have a probability to continue to travel undisturbed and other probabilities to change direction or be absorbed by the media.

There are three measures that characterize absorption and scattering probabilities, the absorption parameter μ_a the scattering parameter μ_s and the probability kernel $g(\mathbf{S}, \mathbf{S}_0)$ expressing the directional change. The first two are measures over the path of photons that travel inside the medium. The third one expresses the conditional possibility that a photon changes direction from \mathbf{S}_0 to \mathbf{S} if it has been scattered.

By definition $1/\mu_a$ expresses the mean value of the exponential probability for the decay of photons that travel inside the medium. Partition of time in steps of Δt implies that for each step photons travel path is $c\Delta t$ where c is the speed of light in the medium.

According to this time partition, the survival – extinction probabilities for the absorption process will be characterized by a Poisson process over the time step with expected value $\mu_\alpha c\Delta t$. The expected population (N) of photons surviving after a small time step Δt will be:

$$N(t + \Delta t) = N(t)P(\text{no absorption}) = N(t) \frac{e^{-\mu_\alpha c\Delta t} (\mu_\alpha c\Delta t)^0}{0!} = N(t)e^{-\mu_\alpha c\Delta t} \Rightarrow$$

$$N(t + \Delta t) \cong N(t)(1 - \mu_\alpha c\Delta t) \text{ if } \mu_\alpha c\Delta t \ll 1 \quad (2)$$

Scattering will be characterized by another Poisson process, implied by the time partition. The population of photons can be grouped in different populations N_0, N_1, N_2, \dots according to the number of scattering events that occurred.

$$N_i(t + \Delta t) = N(t)P(i = \text{scatter events}) = N(t) \frac{e^{-\mu_s c\Delta t} (\mu_s c\Delta t)^i}{i!} \quad (3)$$

To approximate the above process we can use a repeated Bernoulli process using the probability of no scatter event. Bernoulli is the best approximation to Poisson process and a small number of iterations, in the order of ten or less, are enough to approximate the process. The equations will be:

$$N_0(t + \Delta t) \cong N(t)(1 - \mu_s c\Delta t) \text{ if } \mu_s c\Delta t \ll 1 \quad \text{population with no scatter event} \quad (4)$$

$$N_1(t + \Delta t) \cong N(t)\mu_s c\Delta t \text{ if } \mu_s c\Delta t \ll 1 \quad \text{population with one scatter event} \quad (5)$$

Combining the above equations (absorption and scattering) the population will be divided in two types of populations that will survive after time Δt

$$N_0(t + \Delta t) \cong N(t)(1 - \mu_\alpha c\Delta t)(1 - \mu_s c\Delta t) \quad \text{population with no scatter event} \quad (6)$$

$$N_1(t + \Delta t) \cong N(t)(1 - \mu_\alpha c\Delta t)\mu_s c\Delta t \quad \text{population with one scatter event} \quad (7)$$

under the conditions $\mu_\alpha c\Delta t \ll 1$ and $\mu_s c\Delta t \ll 1$

The previous equations give information about the partition of photon population according to the events that occur but neither about the position nor the direction of photons.

Let a point \mathbf{X}_0 around which there is a population of photons travelling at direction \mathbf{S}_0 with speed c . The arising question is what will be the contribution of that to the population at another point \mathbf{X} after time Δt . Naturally the point \mathbf{X} has to be in a distance less or equal to $c\Delta t$.

Population of type N_0 at \mathbf{X}_0 will contribute after Δt to a point \mathbf{X} only if $\mathbf{X} = \mathbf{X}_0 + c\Delta t\mathbf{S}_0$. On the other hand, population of type N_1 at \mathbf{X}_0 will affect every point \mathbf{X} inside the sphere $(\mathbf{X}_0, c\Delta t)$, but propagation direction will rotate from \mathbf{S}_0 to \mathbf{S} . Partitioning the Euclidian space by the typical mesh, based on elementary tetrahedral volumes, or even in equal cubes, will increase the complexity of calculations because of rotation. Rotation of a tetrahedron and transport to another point will produce infinitely many combinations of intersections with the mesh, increasing complexity. Another approach is to select a volume that is invariant under rotation.

Let's define a dense packing of spheres of radius dr that include the volume of interest and denote the centers of the spheres as cloud of points \mathbf{X}_i .

Also let's define as measure the density $J(\mathbf{X}, \mathbf{S}, t)$, the number of photons around point \mathbf{X} that lies inside the sphere (\mathbf{X}, dr) , at time t and travel towards direction \mathbf{S} . Notice that it is not the usual definition of intensity.

The population of type N_0 , around point \mathbf{X}_0 inside the sphere (\mathbf{X}_0, dr) will reach after time Δt at a sphere radius dr with center $\mathbf{B} = \mathbf{X}_0 + c\Delta t\mathbf{S}_0$. The new center \mathbf{B} will almost everywhere lie between some of the previously defined cloud of points according to partition of space \mathbf{R}^3 . Since partition of space has been done by equal volume spheres a first order approximation according to the distance of point \mathbf{X} to the close-neighboring centers will give the measure of the population distribution.

$$\mathbf{B} = \mathbf{X}_0 + c\Delta t\mathbf{S}_0 \quad (8)$$

$$N_{0i}(t + \Delta t) = \frac{(2dr - \|\mathbf{X}_i - \mathbf{B}\|)N_0(t + \Delta t)}{\sum_j^{\|\mathbf{X}_j - \mathbf{B}\| < 2dr} (2dr - \|\mathbf{X}_j - \mathbf{B}\|)} \quad \forall \|\mathbf{X}_i - \mathbf{B}\| < 2dr \text{ and } \mathbf{X}_i, \mathbf{X}_j \in \text{close centers around } \mathbf{B} \quad (9)$$

Or the contribution of population N_0 of sphere \mathbf{X}_0 to close-neighboring centers \mathbf{X}_i around sphere \mathbf{B} with direction \mathbf{S}_0 will be

$$J_0(\mathbf{X}_i, \mathbf{S}_0, t + \Delta t) = \frac{(2dr - \|\mathbf{X}_i - \mathbf{X}_0 - c\Delta t\mathbf{S}_0\|)(1 - \mu_\alpha c\Delta t)(1 - \mu_s c\Delta t)}{\sum_j^{\|\mathbf{X}_j - \mathbf{X}_0 - c\Delta t\mathbf{S}_0\| < 2dr} (2dr - \|\mathbf{X}_j - \mathbf{X}_0 - c\Delta t\mathbf{S}_0\|)} J(\mathbf{X}_0, \mathbf{S}_0, t) \quad (10)$$

$\forall \|\mathbf{X}_i - \mathbf{X}_0 - c\Delta t\mathbf{S}_0\| < 2dr \text{ and } \mathbf{X}_i, \mathbf{X}_j \in \text{close centers around } \mathbf{B}$

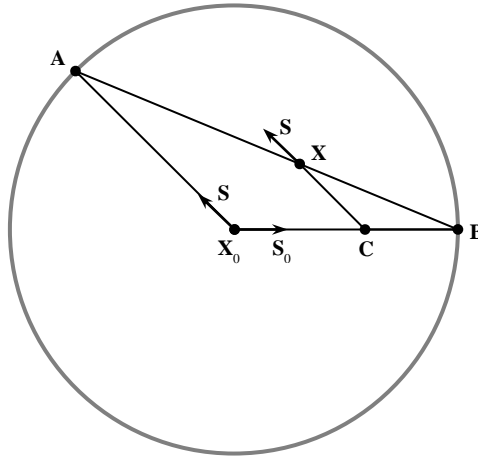


Figure 1. Photon population position after time Δt .
Population N_0 will reach point \mathbf{B} . N_1 will turn from \mathbf{S}_0 to \mathbf{S} at \mathbf{C} to reach point \mathbf{X} .

A part of photon population N_1 that travels to direction \mathbf{S}_0 from point \mathbf{X}_0 will reach point \mathbf{X} after time Δt and this part will have only one direction \mathbf{S} , as illustrated in [Figure 1](#). This is implied by the condition that the travelling path is equal to $c\Delta t$ and only one change of direction is accepted.

$$\|\mathbf{X}_0\mathbf{C}\| + \|\mathbf{CB}\| = \|\mathbf{X}_0\mathbf{C}\| + \|\mathbf{CX}\| = c\Delta t \Rightarrow \|\mathbf{CB}\| = \|\mathbf{CX}\| \quad (11)$$

Triangle \mathbf{CBX} is isosceles and since $\mathbf{B}, \mathbf{X}, \mathbf{X}_0, \mathbf{S}_0$ are fixed so does point \mathbf{C} and direction \mathbf{S} . Since there is one to one correspondence between the pairs $(\mathbf{X}_0, \mathbf{S}_0)$ and (\mathbf{X}, \mathbf{S}) a function can be constructed that connects the directions \mathbf{S}_0 and \mathbf{S} for fixed time step Δt and points \mathbf{X}_0, \mathbf{X} .

This function can be computed solving the following system of vector equations.

$$\left. \begin{array}{l} \mathbf{A} = \mathbf{X}_0 + c\Delta t\mathbf{S} \\ \mathbf{B} = \mathbf{X}_0 + c\Delta t\mathbf{S}_0 \\ \mathbf{B} = k(\mathbf{X} - \mathbf{A}) + \mathbf{A} \quad k \geq 0 \\ \mathbf{S}_0, \mathbf{S} \text{ unit vectors} \end{array} \right\} \Rightarrow \left. \begin{array}{l} \mathbf{B} - \mathbf{A} = c\Delta t(\mathbf{S}_0 - \mathbf{S}) \\ \mathbf{B} - \mathbf{A} = k(\mathbf{X} - \mathbf{X}_0 - c\Delta t\mathbf{S}) \\ \mathbf{B} - \mathbf{X}_0 = k(\mathbf{X} - \mathbf{X}_0 - c\Delta t\mathbf{S}) + \mathbf{X}_0 + c\Delta t\mathbf{S} - \mathbf{X}_0 \end{array} \right\} \Rightarrow$$

$$\left. \begin{array}{l} c\Delta t(\mathbf{S}_0 - \mathbf{S}) = k(\mathbf{X} - \mathbf{X}_0 - c\Delta t\mathbf{S}) \\ \|\mathbf{B} - \mathbf{X}_0\|^2 = k^2\|(\mathbf{X} - \mathbf{X}_0 - c\Delta t\mathbf{S}) + c\Delta t\mathbf{S}\|^2 = (c\Delta t)^2 \end{array} \right\} \Rightarrow$$

$$\left. \begin{array}{l} c\Delta t(\mathbf{S}_0 - \mathbf{S}) = k(\mathbf{X} - \mathbf{X}_0 - c\Delta t\mathbf{S}) \\ (c\Delta t)^2 = k^2\|(\mathbf{X} - \mathbf{X}_0 - c\Delta t\mathbf{S})\|^2 + 2k(\mathbf{X} - \mathbf{X}_0 - c\Delta t\mathbf{S}) * (c\Delta t\mathbf{S}) + (c\Delta t)^2\|\mathbf{S}\|^2 \end{array} \right\} \Rightarrow$$

$$\left. \begin{array}{l} c\Delta t(\mathbf{S}_0 - \mathbf{S}) = k(\mathbf{X} - \mathbf{X}_0 - c\Delta t\mathbf{S}) \\ k = \frac{-2(\mathbf{X} - \mathbf{X}_0 - c\Delta t\mathbf{S}) * (c\Delta t\mathbf{S})}{\|(\mathbf{X} - \mathbf{X}_0 - c\Delta t\mathbf{S})\|^2} \end{array} \right\} \Rightarrow \mathbf{S}_0 = \mathbf{S} - \frac{2(\mathbf{X} - \mathbf{X}_0 - c\Delta t\mathbf{S}) * (\mathbf{X} - \mathbf{X}_0 - c\Delta t\mathbf{S}) * \mathbf{S}}{\|(\mathbf{X} - \mathbf{X}_0 - c\Delta t\mathbf{S})\|^2} \quad (12)$$

Note that because of the symmetry of the equations, the inverse relation is easily calculated. But change of direction has equal probability to occur over time Δt . So the population of photons with the new direction \mathbf{S} will be uniformly distributed over the space around the line segment \mathbf{AB} . The expected part of the population of photons that will change direction from \mathbf{S}_0 to \mathbf{S} is given by the kernel $g(\mathbf{S}, \mathbf{S}_0)$. So the population $g(\mathbf{S}, \mathbf{S}_0)N_1(t + \Delta t)$ will be uniformly distributed around the segment \mathbf{AB} . According to our previous definition of photon density and the equal distribution around the volume defined by the line segment and dr the following relation will be reached, where $J_{X,S}$ is the density of the number of photons in the volume around the line segment.

$$\iiint_{V(\mathbf{AB}, dr)} J_{X,S} dV = g(\mathbf{S}, \mathbf{S}_0)N_1(t + \Delta t) \Rightarrow \quad (13)$$

$$J_{X,S} \iiint_{V(\mathbf{AB}, dr)} dV = g(\mathbf{S}, \mathbf{S}_0)N(t)(1 - \mu_\alpha c\Delta t)\mu_s c\Delta t \quad (14)$$

So the contribution of our measure from point \mathbf{X}_0 and direction \mathbf{S}_0 will be:

$$J_{X,S}(\text{cylinder Vol}(\mathbf{AB}, dr) + \text{half spheres } dr \text{ at points } \mathbf{A}, \mathbf{B}) = J(\mathbf{X}_0, \mathbf{S}_0, t)g(\mathbf{S}, \mathbf{S}_0)(1 - \mu_\alpha c\Delta t)\mu_s c\Delta t \Rightarrow$$

$$\left. \begin{array}{l} J_{X,S} \left(\pi dr^2 \|\mathbf{AB}\| + \frac{4}{3} \pi dr^3 \right) = J(\mathbf{X}_0, \mathbf{S}_0, t)g(\mathbf{S}, \mathbf{S}_0)(1 - \mu_\alpha c\Delta t)\mu_s c\Delta t \\ \|\mathbf{AB}\| = \sqrt{2}c\Delta t(1 - \mathbf{S} * \mathbf{S}_0) \end{array} \right\} \Rightarrow$$

$$J_{X,S} = \frac{g(\mathbf{S}, \mathbf{S}_0)(1 - \mu_\alpha c\Delta t)\mu_s c\Delta t}{\left(\pi dr^2 \sqrt{2}c\Delta t(1 - \mathbf{S} * \mathbf{S}_0) + \frac{4}{3} \pi dr^3 \right)} J(\mathbf{X}_0, \mathbf{S}_0, t) \quad (15)$$

Using the definition of our measure of density as the number of photons inside a sphere (\mathbf{X}, dr) the density of photons at point-center \mathbf{X} directed to \mathbf{S} at time $t + \Delta t$ after one change of direction will be:

$$J_1(\mathbf{X}, \mathbf{S}, t + \Delta t) = J_{X,S} * V_{\text{sphere } dr} = \frac{g(\mathbf{S}, \mathbf{S}_0)(1 - \mu_\alpha c\Delta t)\mu_s c\Delta t}{\frac{3\sqrt{2}c\Delta t(1 - \mathbf{S} * \mathbf{S}_0)}{4dr} + 1} J(\mathbf{X}_0, \mathbf{S}_0, t) \quad (16)$$

The space of travelling direction \mathbf{S} has to be partitioned for calculation purposes. A partition with good symmetry can be constructed using as basis the icosahedron, as all its faces are equilateral triangles (other rules can be applied like Lebedev points[37]). Using as fixed directions the nodes of the icosahedron, densities of arbitrary directions can be calculated by a barycentric interpolation or other interpolation scheme. Let \mathbf{S}_j be the fixed directions then

$$J(\mathbf{X}_0, \mathbf{S}_0, t) = \sum_j \frac{W_j}{\sum_k W_k} J(\mathbf{X}_0, \mathbf{S}_j, t) \text{ where } W_k, W_j \text{ are the barycentric weights} \quad (17)$$

In the case of icosahedron or partitions of it (where each facet is subdivided into smaller equilateral triangles, the sphere is partitioned by triangles so the above equation gets simplified to:

$$J(\mathbf{X}_0, \mathbf{S}_0, t) = \frac{a}{a+b+c} J(\mathbf{X}_0, \mathbf{S}_a, t) + \frac{b}{a+b+c} J(\mathbf{X}_0, \mathbf{S}_b, t) + \frac{c}{a+b+c} J(\mathbf{X}_0, \mathbf{S}_c, t) \quad (18)$$

where a, b, c are distances from directions $\mathbf{S}_a, \mathbf{S}_b, \mathbf{S}_c$ that enclose direction \mathbf{S}_0

Using the previous equation that relates the direction \mathbf{S}_0 and \mathbf{S} setting \mathbf{S} as \mathbf{S}_j from the fixed directions and using the first order approximation defined above, the contribution of density at point $\mathbf{X}_i, \mathbf{S}_j$ from $\mathbf{X}_0, \mathbf{S}_0$ can therefore be calculated. This is the first approach to the computational solution for population N_1 in DRTS.

A second superior approach is to calculate the density at close-neighboring centers \mathbf{X}_i around line segment \mathbf{AB} from $J_1(\mathbf{X}, \mathbf{S}, t + \Delta t)$ using first order approximation according to the distance of centers from \mathbf{AB} . The contribution of population type 1 at point – direction $\mathbf{X}_i, \mathbf{S}_j$ from $\mathbf{X}_0, \mathbf{S}_0$ after time Δt will be

$$J_1(\mathbf{X}_i, \mathbf{S}_j, t + \Delta t) = g(\mathbf{S}_j, \mathbf{S}_0) (1 - \mu_\alpha c \Delta t) \mu_s c \Delta t \frac{2dr - d(\mathbf{X}_i, \mathbf{AB})}{\sum_k^{d(\mathbf{X}_k, \mathbf{AB}) < 2dr} (2dr - d(\mathbf{X}_k, \mathbf{AB}))} J(\mathbf{X}_0, \mathbf{S}_0, t) \quad (19)$$

when $d(\mathbf{X}_i, \mathbf{AB}) < 2dr$

Where $d(\mathbf{X}_i, \mathbf{AB})$ is the distance of center \mathbf{X}_i from line segment \mathbf{AB} . The summation represents the effective volume of cylinder around \mathbf{AB} and the line segment \mathbf{AB} is defined from:

$$\mathbf{A} = c\Delta t \mathbf{S}_j + \mathbf{X}_0 \text{ and } \mathbf{B} = c\Delta t \mathbf{S}_0 + \mathbf{X}_0 \quad (20)$$

The last one approximation scheme preserves the population of photons since the summation of weights is equal to one. On the other hand there is a possibility that some centers \mathbf{X}_i will have no intensity if the partition of directions is not dense enough, however this can be circumvented by using the limitation:

$$c\Delta t \|\mathbf{S}_j - \mathbf{S}_{j+1}\| < 2dr \quad (21)$$

The above inequality can be used as a rule of thumb to avoid the problem of zero densities. The left term represents the arc length on the sphere $c\Delta t$ between two adjusted directions.

In comparison, the first approach expressed in equation (18), which is based on arbitrary directions, does not suffer from zero densities, but has the serious disadvantage that the summation of populations after Δt may not be equal to the starting population decreased by the absorption.

Since the photons traveling inside the media are independent, the whole contribution at a center – direction will be the summation of all contributions from all centers – directions that lie in the sphere of radius $c\Delta t$. To organize calculations our measure will be represented by a vector $\mathbf{J}_{\mathbf{X}, \mathbf{S}}$ and the contribution according to the previous discussion will be described by a square matrix \mathbf{A} . So the time evolution of photons travelling inside scattering absorbing media will be expressed by the system:

$$J(\mathbf{X}, \mathbf{S}, t + \Delta t) = \mathbf{A} J(\mathbf{X}, \mathbf{S}, t) \text{ or } J(\mathbf{X}, \mathbf{S}, t + \Delta t) = (1 - \mu_\alpha c \Delta t) \mathbf{A}_1 J(\mathbf{X}, \mathbf{S}, t) \quad (22)$$

Since the factor $(1 - \mu_\alpha c\Delta t)$ is constant, matrix \mathbf{A}_1 will characterize the system. These matrices have some important properties:

- Matrix \mathbf{A} and \mathbf{A}_1 is sparse. This is easily seen since every $J_{\mathbf{X},\mathbf{S}}$ can be affected only by other centers that lies within the sphere $(\mathbf{X}, c\Delta t)$.
- The summation of every column of \mathbf{A}_1 is 1 (because of population conservation).
- Every number in \mathbf{A} and \mathbf{A}_1 is positive less or equal to one or zero. This comes from the fact every element in arrays express a possibility.
- The diagonal is zero. Diagonal elements correspond to photons returning at the same center and same direction. But after time Δt no photons will be in the same place except photons that have backward direction that travel $c\Delta t/2$ and return. This is due to the fact that only one change of direction is accepted. This can also be verified by the equation that relates \mathbf{S}_0 and \mathbf{S} .
- The matrices are irreducible under the condition that every center \mathbf{X}_i has at least one direction \mathbf{S}_j such that the line segment $\mathbf{X}_i, \mathbf{X} = \mathbf{X}_i + \frac{3}{2}c\Delta t\mathbf{S}_j$ lies inside the volume of interest and the volume is connected.

To prove the last one let's create a directed graph with vertices $J_{\mathbf{X}_i\mathbf{S}_j}$ and direct edges from $J_{\mathbf{X}_i\mathbf{S}_j}$ to $J_{\mathbf{X}_k\mathbf{S}_l}$ if there is a contribution of photons from $\mathbf{X}_i, \mathbf{S}_j$ to $\mathbf{X}_k, \mathbf{S}_l$; this means that the corresponding value in the array is positive. Arrays \mathbf{A} and \mathbf{A}_1 are irreducible if and only if there is a path from every vertex to any vertex, or the graph is strongly connected. Starting from a vertex $J_{\mathbf{X}_0\mathbf{S}_0}$ under the first condition there should exist a point $\mathbf{X}_A = \mathbf{X}_0 + c\Delta t\mathbf{S}_j$ inside the volume. According to the approximation of photon population of type 1 there will be some photons that come from $J_{\mathbf{X}_0\mathbf{S}_0}$ and change direction from \mathbf{S}_0 to \mathbf{S}_j and distribute to centers \mathbf{X}_l with direction \mathbf{S}_j near the point $\mathbf{X}_A = \mathbf{X}_0 + c\Delta t\mathbf{S}_j$. From centers \mathbf{X}_l and direction \mathbf{S}_j there will be a connection to the same centers \mathbf{X}_l and direction $-\mathbf{S}_j$ since the point $\mathbf{X}_B = \mathbf{X}_i + \frac{3}{2}c\Delta t\mathbf{S}_j = \mathbf{X}_l + \frac{1}{2}c\Delta t\mathbf{S}_j$ lies inside volume. From centers \mathbf{X}_l and direction $-\mathbf{S}_j$ we reach center \mathbf{X}_0 . Since this center is at distance $c\Delta t$ at direction $-\mathbf{S}_j$ there is distribution of population type 1 to every direction. So starting from vertex $J_{\mathbf{X}_0\mathbf{S}_0}$ we can reach every vertex of type $J_{\mathbf{X}_0\mathbf{S}_i}$. The transition path is

$$J_{\mathbf{X}_0\mathbf{S}_0} \xrightarrow{g(\mathbf{S}_j, \mathbf{S}_0)} J_{\mathbf{X}_0+c\Delta t\mathbf{S}_j, \mathbf{S}_j} \xrightarrow{g(-\mathbf{S}_j, \mathbf{S}_j)} J_{\mathbf{X}_0+c\Delta t\mathbf{S}_j, -\mathbf{S}_j} \xrightarrow{g(\mathbf{S}_i, -\mathbf{S}_j)} J_{\mathbf{X}_0\mathbf{S}_i} \quad (23)$$

Since by starting from a center and specific direction we can always reach any direction of the same center, it is enough to prove that starting from a center \mathbf{X}_0 we can reach any center \mathbf{X}_k . This can be proved by the following procedure.

From center \mathbf{X}_0 there is a path to every center that lies inside sphere $\mathbf{X}_0, c\Delta t$. If the center \mathbf{X}_k has been reached the proof is completed, otherwise we "mark" the boundary centers, remove the remaining centers inside the sphere and repeat the procedure for the marked centers. Since the volume is connected and the remaining volume is smaller, the algorithm will end and will reach center \mathbf{X}_k . Therefore this concludes the sought proof that matrices \mathbf{A} and \mathbf{A}_1 are irreducible.

3. An approach to modeling the effects of the sources and boundary conditions in media with multiple refractive indices

A general dynamic system calculation method like DRTS in order to be meaningful, it should be universally applicable in a multitude of physical phenomena. In our case this includes boundary conditions, different media, sources and phenomena like specular or diffusive reflection, refractive deflection, etc. and,

finally integrating the measurement process for these phenomena. In this section we outline the approach for introducing all relevant phenomena and processes in the DRTS methodology in a consistent way. The analytic expression in each case depends on the mathematical description or modeling and on the detailed properties of the examined materials, measurement probes, etc.

3.1. The effect of the sources

Typically sources of light are described with a time and space – dependent power flow (intensity) function having a defined volume or surface distribution. To incorporate this information in our dynamic system modeling (DRTS) it must first be expressed as a spatial – directional distribution of photons for every single time step Δt . This is necessary as our measure J counts the number of photons inside a volume of a sphere (X, dr) at distinct points of time $k\Delta t$, where conversion of energy to number of photons can be done using $E = hv$. Using the previously defined space and direction partitions, it is possible to translate the source influence into photon-population contributions inside the spheres and angular directions. To calculate the contribution of sources, the number of photons that are produced or inserted between in the time interval $[k\Delta t, (k + 1)\Delta t]$ has to be expressed. Also the position and direction of them at time $(k + 1)\Delta t$ have to be determined. These source contributions, because of the discretized system description, will be expressed by a correlation matrix of photon presence inside the specific spheres and direction angles due to their outflow from the sources. Therefore in the general case our system will be described by a system:

$$J(X, S, t + \Delta t) = A J(X, S, t) + B P(X, S, t) \quad (24)$$

where $P(X, S, t)$ is the discrete source vector of photon production, and B is the correlation array with our positional centers X_i , directions S_j and time. Here, for an accurate calculation, the time-partition of the source function should be implemented in shorter time intervals dr/c .

3.2. Media boundaries and measurement processes

In this section the processes related to photons crossing boundaries between different physical media as well as the final measurement of the emerging photon populations will be described. In the most complicated scenario the media will differ in their absorption and diffusion parameters and refractive index. The treatment now involves a 2 – step process for the photons passing through the boundary within the time interval Δt . During the first step the propagation is calculated until the photon reaches the media interface in time shorter than Δt . At this point the relevant photon population is considered as a new Dirac source for the second medium and its propagation for the remaining time (till the end of interval Δt) is similarly evaluated using the new medium parameters. This method has the advantage that it does not essentially modify the previous methodology but simply makes elements of A matrix more complicated to evaluate. It should be noted, however, that this evaluation should be performed only once.

Photons passing through a surface with a change of velocity will produce specular reflection and deflection. These phenomena must be included in our calculations.

Since the problem is transformed to geometrical problem only a brief outline of the solution will be given. Photons will travel over the path X_0C in accordance to the equations given in previous section by replacing the path $c\Delta t$ with the actual one $\|X_0C\|$. At point C two new sources will be produced, one at direction S^r that will obey the reflection laws and one at S^t that will obey refraction laws. The effect produced at time $t + \Delta t$ from these sources can be easily calculated since they are of Dirac type. In the second figure is it shown that the part $\frac{\|c'\|}{\|X_0C\|}$ of population N_1 that was turned from S_0 to S will be distributed to line segment $X'X''$ with direction S^r because of reflection and the transmitted part will be distributed over X^0X'' with direction S^o . The absorption of this transmitted part will be proportional to the path the photons travel inside the volume.

This can be easily calculated, because of linearity, by computing the effects at the extreme points X^o and X'' . Population type N_1 produced by the Dirac type source after reflection may hit one more time the surface depending on the direction of a possible subsequent scattering. Since at very short time intervals only one change of direction is possible, there will be no further hits on the media interface in time Δt . So these two steps conclude the photon propagation calculation giving again geometrical interpretations to the dynamic system evolution.

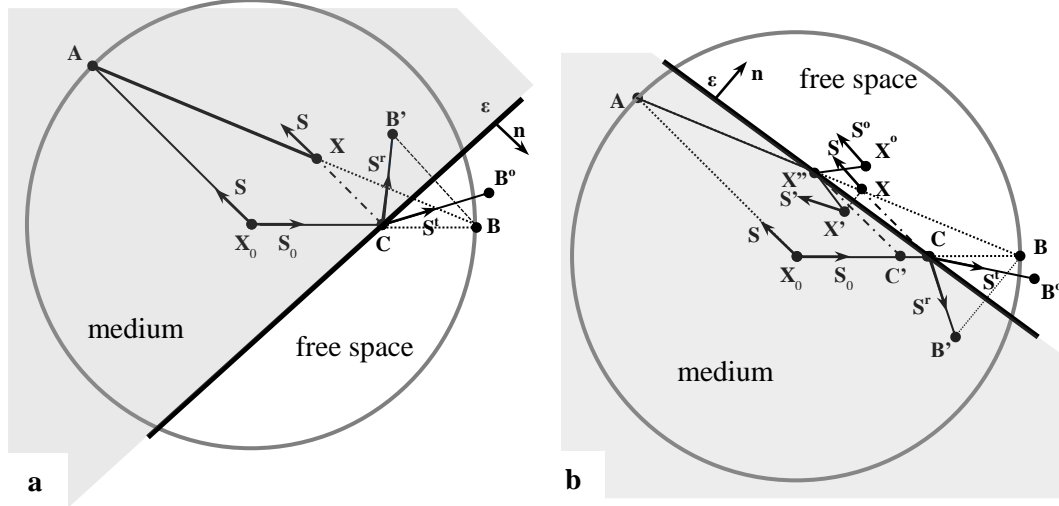


Figure 2. Photon population position after time Δt when reaching surface of different media
a. At point C two rays will be created, reflected S^r and transmitted S^t .
b. Reflection of population N_1 , population will be distributed at $X'X''$ (reflected) and $X''X^o$ (transmitted).

Measurements especially in a laboratory environment involve finite volumes so boundary effects have to be investigated in accordance with a possible measurement system. Sensors of random photons are based on photon count (as PMT, Photodiode) or in energy absorption (temperature type), however both types can be treated as photon count sensors. On the other hand any sensor response is based on a time integral even if the time interval is very small. The response of any measurement system will be proportional to photons that reach the sensor in a certain time interval – time window. By calculating the photon propagation via the external media boundary into the open space at the conclusion of a time interval Δt , in a manner analogous to that described above for the case of dissimilar media, we can obtain full information for the photon population in a volume of thickness $c^o \Delta t$ that embraces all the medium under investigation. Subsequently, photons that flow out of the boundary of this volume in the appropriate directions will reach the sensor at a time that depends on the relative positions of photons and sensor. Taking into account that the speed of light is constant in the space between the volume boundary and the measurement system and the fact that there is no scattering in this space, we have the opportunity to separate the information given from the volume under examination and the measurement system.

To this purpose, let's extend the partition of R^3 by considering closely – packed spheres (X^o, dr) outside the boundary of the measure volume till a distance $c^o \Delta t$, where c^o is the velocity of photons in the medium (typically air) outside the studied scattering – absorptive volume. A system will respond with a measure $M(t)$ to the number of photons P^o that arrive at the sensor according to a time and directional sensitivity $G(S, t)$

$$M(t) = \iint_{s, t-w}^{t+w} G(S, t) P^o dt ds \cong \sum_{s_i} \sum_{t-w}^{t+w} G(S_i, t_j) P^o \Delta s \Delta t = \sum_{\substack{\text{extended} \\ \text{volume}}} F(X_i^o, S_j, k\Delta t) J(X_i^o, S_j, k\Delta t) \quad (25)$$

where $F(X_i^o, S_j, k\Delta t)$ includes the effects of sensor time – response over the time window interval ($2w$)

The time delay that photons have to reach the sensor starting from position X_i^o and $G(\mathbf{S}, t)$ is the directional sensitivity of the sensor. It is clear, from previous analysis, that the independent information given from the volume under investigation, is described by the distribution $J(X_i^o, \mathbf{S}_j, k\Delta t)$ of photons in the extended volume which can now be calculated. Our system will have the form:

$$J(\mathbf{X}, \mathbf{S}, t + \Delta t) = \mathbf{A} J(\mathbf{X}, \mathbf{S}, t) + \mathbf{B} P(\mathbf{X}, \mathbf{S}, t) \quad (26)$$

$$J(\mathbf{X}^o, \mathbf{S}, t + \Delta t) = \mathbf{C} J(\mathbf{X}, \mathbf{S}, t) + \mathbf{D} J(\mathbf{X}^o, \mathbf{S}, t) \quad (27)$$

where \mathbf{C} is the matrix that correlates the internal volume measure $J(\mathbf{X}, \mathbf{S}, t)$ with the extended volume and \mathbf{D} is a possible relation of photons in extended volume (usually a simple positional translation). Combining the internal and external state vector in a new one the system will be transformed to one equation which includes all the volume. New symbols are used since they are referred to the whole volume.

$$J(\mathbf{X}^a, \mathbf{S}, t + \Delta t) = \mathbf{A}' J(\mathbf{X}^a, \mathbf{S}, t) + \mathbf{B}' P'(\mathbf{X}^a, \mathbf{S}, t) \quad (28)$$

4. Simulation Results

The algorithm from the previous theoretical analysis is summarized according to the following flowchart (Figure 3).

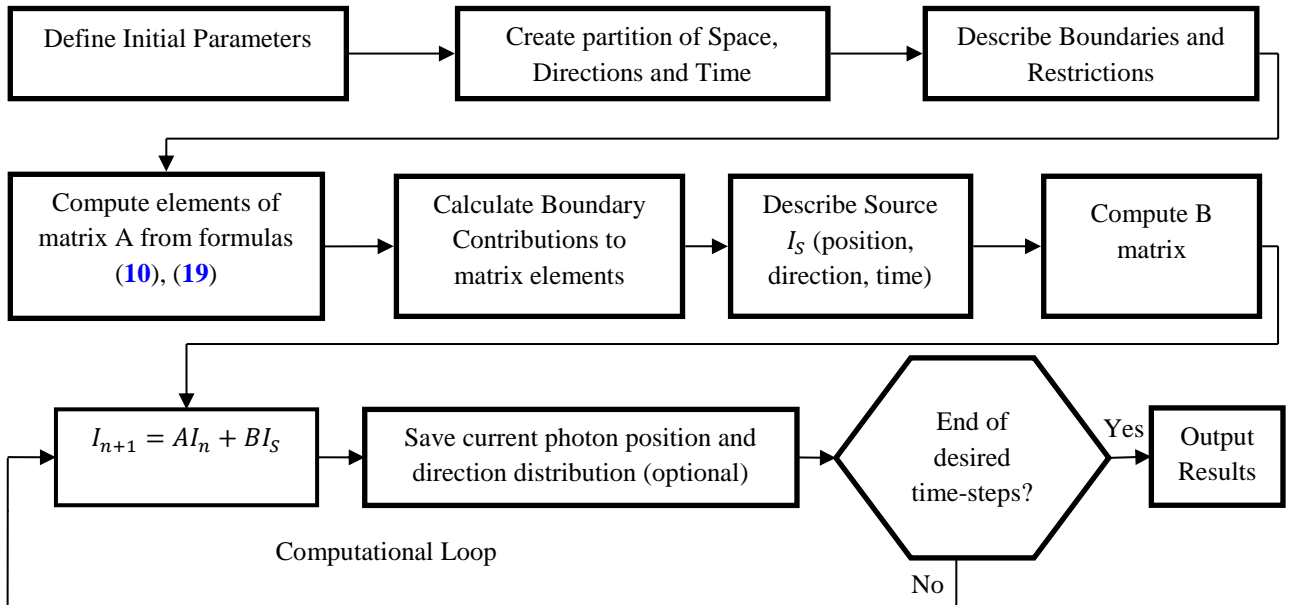


Figure 3. Photon Density in logarithmic scale for a diffusing light pulse inside strongly scattering media and anisotropy factor $g = 0$

This algorithm was implemented in C# and was applied for the calculation of propagation of ultra-fast photon pulses in various scattering and absorbing media. For testing purposes, initial simulations assumed an optically uniform medium shaped as rectangular box. The light source is a collimated directional beam propagating along the y-axis (“horizontal” axis in our figures and video) impinging at the center of the $y=0$ plane. The partition of the media volume was $100 \times 100 \times 100$ close-packing of equal spheres. Directional partition was implemented with the Lebedev rule using 86 directions. To fulfill the requirements of equations (6) and (7) and according to the optical properties of the medium (μ_a, μ_s), a suitable time step had to be

defined. In our simulations $\Delta t = 0.1/(c \cdot \max\{\mu_a, \mu_s\})$ was selected. The angular scattering dependence of single scattering events, was approximated by the Henyey-Greenstein scattering function. In the simulation results below, two cases are presented, one for isotropic scattering ($g = 0$) and one for the forward scattering ($g = 0.7$), with the latter being a typical value for biological tissues. The spatial dimension of the input photon source here occupies a “cuboctahedron” volume of 13 neighboring spheres (a central sphere plus 12 closest-neighbor spheres) positioned at the center of the $y = 0$ face of the medium. A number of photons are emitted at $t = 0$ from all source cells along the y -direction, simulating a single-directional delta-function distribution over time. This source should be viewed as an ultra-short incoherent light pulse, in order to avoid complications arising from interference phenomena, which have not yet been included in our model. Also, for simplicity, no reflection effects from the medium external surfaces were considered in these simulation runs. Numerical results are depicted below in figures and graphs, where all data are represented in logarithmic scales because of the extreme spread in data values, typically 10^{20} .

4.1. Simulating strongly scattering, weakly absorbing, isotropic homogeneous media

For a strongly scattering and weakly absorbing medium ($\mu_s/\mu_a = 100$) with isotropic scattering, the total photon density distribution for three different time frames ($t_1 = 2\Delta t, t_2 = 6\Delta t, t_3 = 15\Delta t$) is shown in Figure 4 sequence. It should be noted that all calculations were done in 3 spatial dimensions, from which these 2D graphs were subsequently extracted for the sake of clarity of representation. Photon densities are represented with pseudo-colors covering a 10^{20} dynamic range according to the explanatory logarithmic color scale at the right side.

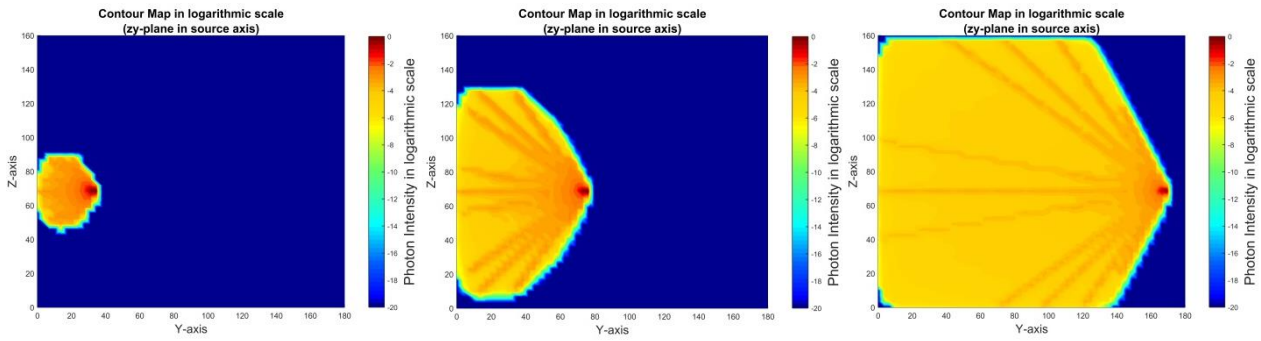


Figure 4. Photon Density in logarithmic scale for a diffusing light pulse inside strongly scattering media and anisotropy factor $g = 0$, at three different time frames ($t_1 = 2\Delta t, t_2 = 6\Delta t, t_3 = 15\Delta t$).

The red tip of the distribution corresponds to un-scattered photons traveling at the speed of light ($c=c_0/n$) in the medium, while other parts of the distribution correspond to scattered photons towards all possible directions. The line-patterns inside the distribution (in the form of diverging “fan-out” trails) are simulation artifacts due to the finite number of directions (86) considered in our angular-space partition.

A full 3D frame of the same sequence is included here in Figure 5, to demonstrate the shape of the propagating photon distribution as it diffuses in the scattering medium.

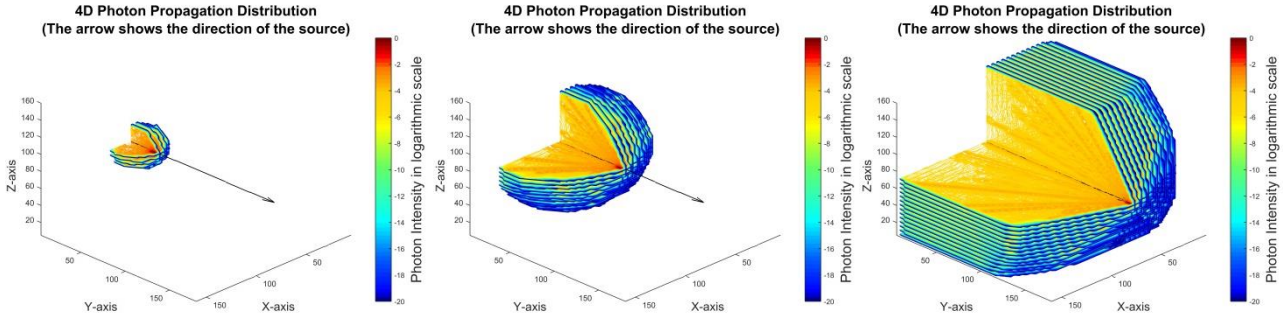


Figure 5. Time propagation of Photon Density in 3D for a diffusing light pulse inside strongly scattering media, The arrow indicates the source direction, in three different time frames ($t_1 = 2\Delta t, t_2 = 6\Delta t, t_3 = 15\Delta t$).

The following **Figure 6** and **Figure 7** sequences show the spatial distribution of photons traveling along a single direction, specifically either along the original source y-direction (0°) or perpendicular to that ($+90^\circ$ angle), in the same material as above.

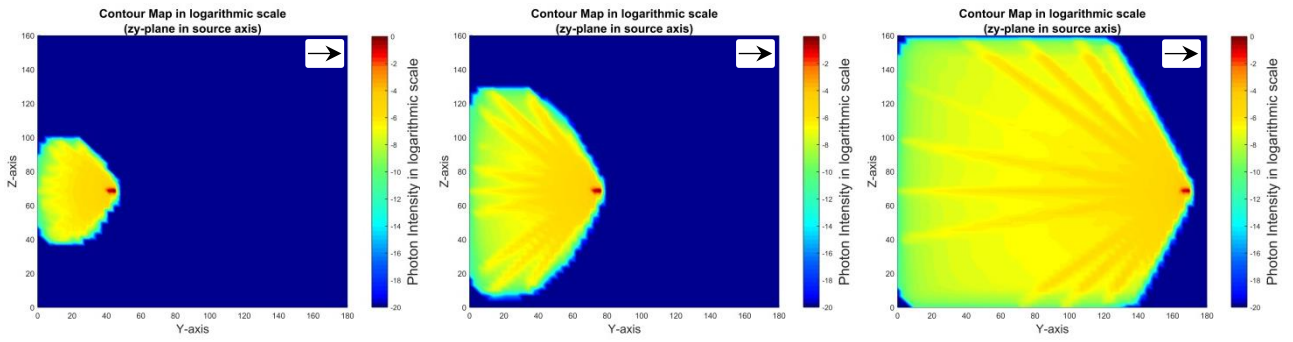


Figure 6. Photon populations traveling exclusively along the original source direction (y-axis) - indicated by the arrow at top right corner - at three different time frames ($t_1 = 2\Delta t, t_2 = 6\Delta t, t_3 = 15\Delta t$).

In **Figure 6** sequence we have isolated the photon populations traveling exclusively along the y-axis at each time frame (indicated by arrow at top right corner of each contour map image). These photons happen to be either yet unscattered (population at the front tip of the distribution), or have gone through a suitable number of scatterings (at least 2) that allowed them to resume in the y-axis direction.

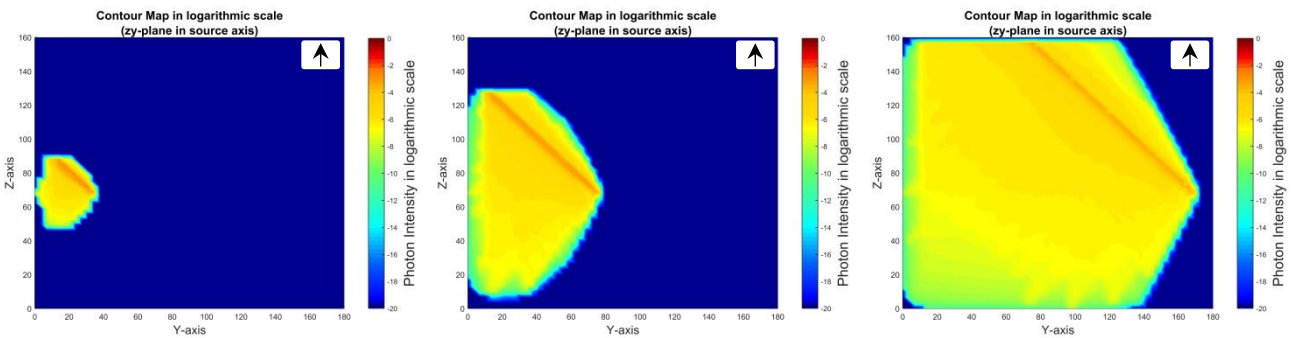


Figure 7. Photon populations traveling along the positive z-axis (i.e. at 90° to the original source y-direction) - indicated by the arrow at top right corner - at three different time frames ($t_1 = 2\Delta t, t_2 = 6\Delta t, t_3 = 15\Delta t$).

Correspondingly, in **Figure 7** sequence we have isolated, at each time frame, the photon populations traveling along the +z-axis, perpendicular to the original y-axis source direction (indicated by the arrow in top right corner of each contour map image). These photons have undergone a suitable number of scatterings (at

least one) that streamed them in the $+90^\circ$ direction. The peak of the photon density is a line representing photons that had undergone only one scattering. This line distribution was expected from the theoretical analysis of section 2, and illustrated in Figure 1.

4.2. Simulating strongly forward scattering, weakly absorbing, isotropic homogeneous media

For a medium with a different forward scattering ($g=0.7$) and same μ_a, μ_s coefficients as before, the photon propagation is plotted in **Figure 8** sequence. The contour map shows, as expected, increased density values in directions closer to the direction of the source.

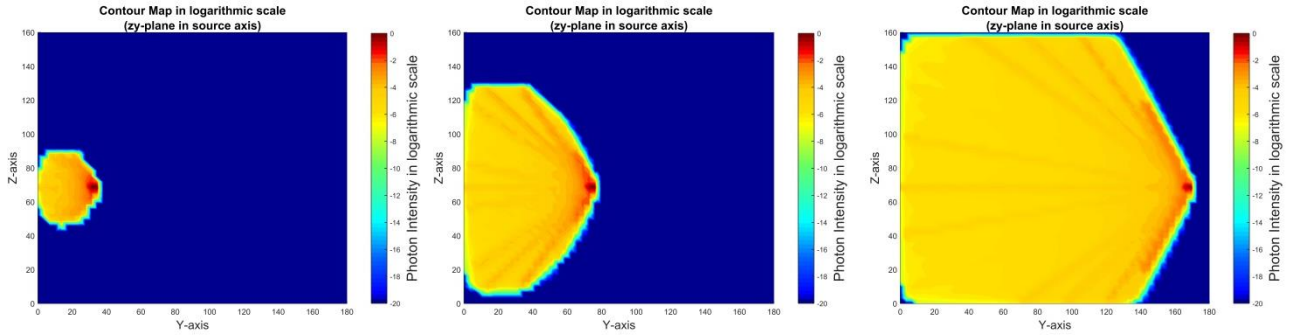


Figure 8. Photon populations for a diffusing light pulse inside strongly scattering media with anisotropy factor $g=0.7$, at three different time frames ($t_1 = 2\Delta t, t_2 = 6\Delta t, t_3 = 15\Delta t$). The density in directions closer to the direction of the source is increased compared to Figure 4 (red area around wave front).

4.3. Simulating strongly scattering, strongly absorbing, isotropic homogeneous media

For a higher absorption coefficient value ($\mu_a/\mu_s = 4$) and isotropic scattering medium, the analogous propagation of total photon population distribution at different times is shown in the picture sequence of **Figure 9**.

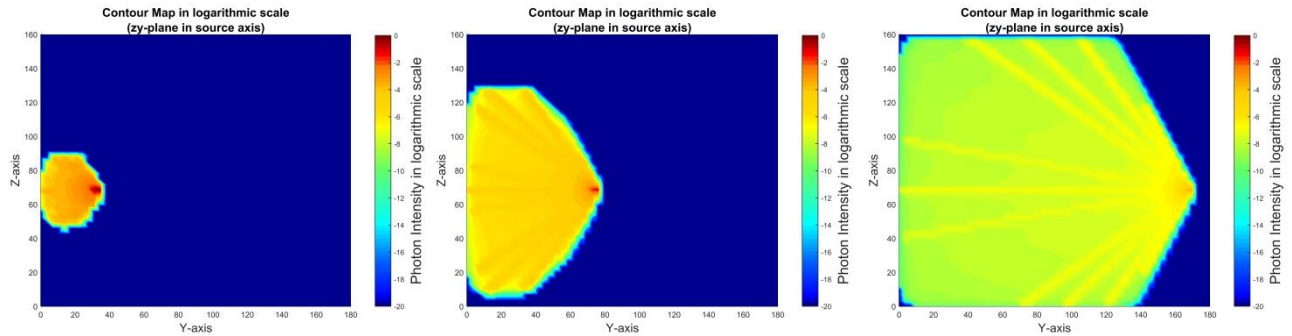


Figure 9. Photon populations for a diffusing light pulse inside strongly absorbing media with isotropic scattering $g=0$, at three different time frames ($t_1 = 2\Delta t, t_2 = 6\Delta t, t_3 = 15\Delta t$).

4.4. Simulating a measurement system

As explained in paragraph 3.2, in equation (25), a measurement system will respond to photon population, time interval and the characteristics of the sensor. Since in our simulation no special sensor was assumed, a hypothetical response of a single-directional point detector is presented in **Figure 10**.

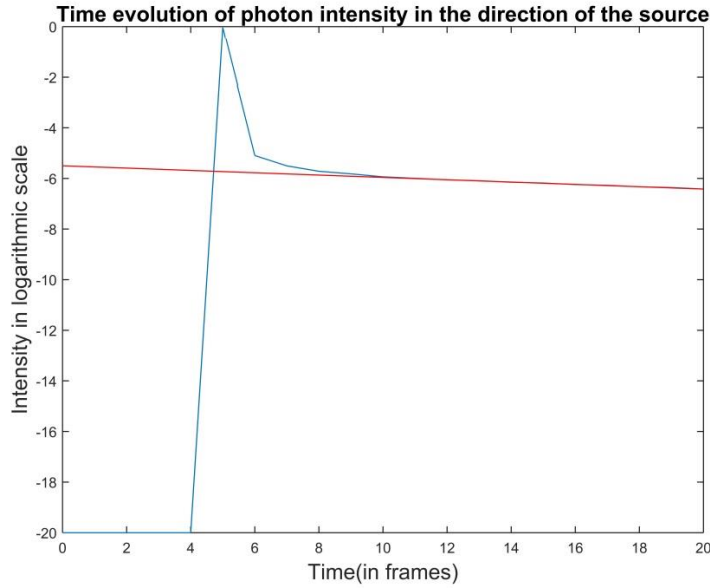


Figure 10. Time evolution of photon intensity at a point lying along the source direction. The red line indicates the integro-differential RTE solution, which cannot describe the spike produced by the light front at the sensor position. The blue line indicates the DRTS solution, which accurately represents the actual physical phenomenon.

The hypothetical sensor was positioned on the source direction axis at a distance of $1/5$ of the media length and assumed to respond only to photons traveling along that direction. The graph shows the surge of the light-front intensity arriving at the sensor on the fifth time step, corresponding to unscattered photons. Subsequently, the diffused photon population arrives, with the time-distribution gradually tailing-off exponentially. This signal decay is indicated by the straight line (red line in figure) of the log plot, the slope of which determines the combined absorption and scattering coefficients, therefore it can be further used to derive the light propagation characteristics of the medium. It should be noted that integro-differential RTE cannot describe the spike produced by the light-front arrival.

5. Discussion: Comparisons and Conclusions

5.1. Comparison of Methods

The new DRTS method was developed as a mathematical and computational tool suitable for solving important physical problems of time-evolution of photon propagation in absorptive and scattering media. Thus it is interesting to discuss this method in comparison with the widely-used RTE and MC. Both DRTS and RTE try to express mathematically the same physical phenomena but they differ in their philosophical points of view. Specifically RTE uses the conventional interpretation of physical phenomenon and vector space by approaching the concept of variation of quantity and space-point via limit to zero and arrives to an integro – differential equation. Then for calculation purposes the solution space of the integro – differential expression is approximated by an infinite functional base. But in a real measurement system neither zero nor infinity can be reached, so large errors are quite possible. On the other hand DRTS tries to avoid these two dangerous domains (limit to zero and infinity) by proceeding via a dynamical system approach. Monte Carlo methods and DRTS employ the exact statistical physical phenomenon but DRTS additionally stores the full material information, in a unique matrix form, that is calculated only once. In contrast MC is not aware of the system behavior and tries to resolve the solution by “throwing dices”, which turns out right only because the expected value will be approximated after a large number of iterations.

Another interesting comparison can be made on the basis of the flexibility aspects. For example, RTE model cannot handle reflection, refraction, non-convex volume shapes (involving re-entry of radiation), spikes, etc. By contrast, MC and DRTS (as previously indicated in section 3) can handle these phenomena and solve these problems under a general and consistent scheme. Specifically, a modified MC method will monitor these phenomena during algorithm iterations, while DRTS incorporates these effects in the single calculation of the system matrix.

Regarding the computational requirements and cost comparison between the three methodologies examined, the following points emerge.

Advantages of DRTS in terms of computational cost become evident once the general flow scheme is considered. The method starts with the elements calculation, equations (10) and (17), of the system matrix A of equation (22), a time- and computation-demanding step, which however will have to be performed (and stored) only once for the whole process. It should also be pointed out that this system matrix A is sparse, a fact that greatly reduces problem complexity, storage requirements and computational cost for the subsequent steps. To calculate the photon-system status on the next step after time Δt has elapsed, it suffices to simply multiply the above system matrix A with the initial system status-vector and add any new source term (equation (24)). The new vector result, after Δt , can be reused on-the-fly in RAM as the starting point for the subsequent step, where matrix A will remain un-altered. All subsequent computational cost will only involve elementary sparse-matrix – vector calculations (without any matrix inversions), all with non-negative numbers. Thus there is absolutely no cause for calculation instabilities.

To demonstrate the superiority of the DRTS method versus the mainstream standard calculation methods (Monte Carlo and Finite Elements – like methods) we consider their comparative practical application in simulations of similar complexity as the test-case problems of the previous section. In these examples, DRTS was programmed and run on a standard PC machine and handled easily the ultra-short light-pulse propagation where photon density was described by a $86 \cdot 10^6$ – elements vector, producing a variety of useful results for any desired time sequence without any instabilities or storage overflow problems.

An equivalent computation by means of Monte-Carlo method, for comparison, would be greatly inferior. For the same number of partition micro-volumes and for the given dynamic range, the required number of iterations with Monte-Carlo algorithms would be at least a hundred times the dynamic range of photon density. In our method the precision of calculation is restricted only by computer precision. In our simulation results a dynamic range of 10^{20} is presented. For this range Monte-Carlo would need at least 10^{22} iterations, which is prohibitively large on standard computer systems. Also worth noting, on every iteration MC has to produce random numbers and calculate exponential or logarithmic probabilities. Such dynamic range is crucial when modeling transient phenomena, as is exactly the case with ultrafast light pulse diffusive propagation. Additionally, as Monte-Carlo methods require summation of all the individual intermediate results to give the final answer, all these data would have to be stored, handled and retrieved, requiring an increase of required system memory. For our particular example, memory requirements for MC would be $86 \cdot 10^6 * time\ steps * 10bytes \approx [time\ steps] * Gb$ (since double precision uses 10bytes of memory). It should be noted that any intermediate results in DRTS are used just once and storage to disk is performed only if results output is desired at that time step, as also indicated in the flowchart. Overall, even for relatively simple problems of low complexity, as presented above, Monte-Carlo calculations demand vast computational costs, related to the required iteration numbers and execution time, and also to the extreme storage requirements.

In comparison with integro-differential models, an equivalent simulation with finite elements would involve a similar number of iterations as with the DRTS above, albeit including matrix-inversion operations at each step, therefore vastly increasing the computational cost. This is due to the fact that approximation

methods assume that the solution to a differential-equation system can be described by a weighted summation of a base functions set, the coefficients of which have to be determined. This leads to a linear equation system, which requires a matrix inversion in every time step. Apart from the computational cost, a harmful side-effect is the potential non-positivity of the solution, which is physically non-acceptable in the case of radiation intensity.

Another computational disadvantage of both RTE approximation methods and MC solutions relates to the difficulty of re-evaluating system response in cases of modified configuration of sources. These methods have to recalculate everything from scratch if any modification is made in the original source positions or directions. On the other hand, in DRTS array \mathbf{A} remains unchanged, and – as typically a light beam occupies very confined spatial dimensions – array \mathbf{B} will be non-zero only for the corresponding elements. The only modification therefore will be array \mathbf{B} and the source vector, equation (24), so the computational cost in DRTS again is comparatively much smaller.

5.2. Conclusions

According to the previous analysis, DRTS presents a novel perspective of thought, a new theory and a concrete method for solution, which offers several important advantages for treating radiation-propagation problems:

- The new method is able to accurately predict the time-dependent evolution of photon flow, even for fast-varying sources. This is important in solving the Optical Tomography “forward problem” in the case of pulsed excitation.
- DRTS can treat problems involving physical limitations or correlations, like quantitative equalities or inequalities, parameter bounds, etc. which can be effectively taken into account during the construction of the system matrices.
- Time-varying parameters can be competently handled by linear approximation since Δt is adequately small. In this case arrays have to be re – estimated over time, so this will only increase the calculation cost.
- The freedom of extension the volume of interest (as in the case of media boundaries and measurement) gives the ability to overcome mathematical difficulties caused by non-convex volumes. In general DRTS is not affected if the volume is enclosed inside a convex one (like a simple cube or a sphere) and simply solves the problem over the new extended regime.
- DRTS uses a dynamical-system formality and provides physical and geometrical interpretations for the system evolution. The basic structure of the method can be enhanced to accept more complicated problems which are closer to the physical reality.
- The DRTS method allows the calculation either of photon population-density or the derivation of directional flow. This can be achieved by simple matrix operations.

Finally, it should be noted that the general philosophy and methodology of “Dynamical Radiative Transfer System” should also be applicable in many scientific areas to calculate other physical phenomena by increasing the variable space, since many differential systems under conditions can be transformed to a similar type of calculations.

Future work will be directed towards DRTS error analysis, detailed modeling of pulsed sources, interference phenomena and application-software development.

References

- [1] Richling S, Meinköhn E, Kryzhevoi N and Kanschat G 2001 Radiative transfer with finite elements *Astronomy & Astrophysics* **380** 776-88
- [2] Kasen D, Thomas R C, Röpke F and Woosley S E 2008 Multidimensional radiative transfer calculations of the light curves and spectra of Type Ia supernovae *Journal of Physics: Conference Series* **125**
- [3] Dos Santos R V and Dickman R 2013 Survival of the scarcer in space *Journal of Statistical Mechanics: Theory and Experiment* **2013**
- [4] Barichello L B and Siewert C E 1998 On the equivalence between the discrete ordinates and the spherical harmonics methods in radiative transfer *Nuclear Science and Engineering* **130** 79-84
- [5] An W, Ruan L M, Tan H P and Qi H 2006 Least-Squares Finite Element Analysis for Transient Radiative Transfer in Absorbing and Scattering Media *Journal of Heat Transfer* **128** 499
- [6] Modest M F and Lei S 2012 The Simplified Spherical Harmonics Method For Radiative Heat Transfer *Journal of Physics: Conference Series* **369** 012019
- [7] Ravishankar M, Mazumder S and Kumar A 2010 Finite-Volume Formulation and Solution of the P₃ Equations of Radiative Transfer on Unstructured Meshes *Journal of Heat Transfer* **132** 023402
- [8] Gorpas D, Yova D and Politopoulos K 2010 A three-dimensional finite elements approach for the coupled radiative transfer equation and diffusion approximation modeling in fluorescence imaging *Journal of Quantitative Spectroscopy and Radiative Transfer* **111** 553-68
- [9] Joshi A, Rasmussen J C, Sevick-Muraca E M, Wareing T A and McGhee J 2008 Radiative transport-based frequency-domain fluorescence tomography *Physics in Medicine and Biology* **53** 2069-88
- [10] Simon E, Foschum F and Kienle A 2013 Hybrid Green's function of the time-dependent radiative transfer equation for anisotropically scattering semi-infinite media *Journal of Biomedical Optics* **18** 015001
- [11] Singh A R, Giri D and Kumar S 2011 Statistical mechanics of stretching of biopolymers *Journal of Statistical Mechanics: Theory and Experiment* **2011**
- [12] Kanschat G, Meinköhn E, Rannacher R and Wehrse R 2009 *Numerical methods in multidimensional radiative transfer*
- [13] Wang L, Jacques S L and Zheng L 1995 MCML—Monte Carlo modeling of light transport in multi-layered tissues *Computer Methods and Programs in Biomedicine* **47** 131-46
- [14] Brinkworth B J and Harris D O 1970 Multiple scattering analysis by diffusion and Monte Carlo methods *Journal of Physics D: Applied Physics* **3** 397-404
- [15] Evans K F 1998 The Spherical Harmonics Discrete Ordinate Method for Three-Dimensional Atmospheric Radiative Transfer *Journal of the Atmospheric Sciences* **55** 429-46
- [16] Ou S-C S and Liou K-N 1982 Generalization of the spherical harmonic method to radiative transfer in multi-dimensional space *Journal of Quantitative Spectroscopy and Radiative Transfer* **28** 271-88
- [17] Ohkubo J and Eggel T 2010 A direct numerical method for obtaining the counting statistics for stochastic processes *Journal of Statistical Mechanics: Theory and Experiment* **2010**
- [18] Fujii H, Okawa S, Yamada Y and Hoshi Y 2014 Hybrid model of light propagation in random media based on the time-dependent radiative transfer and diffusion equations *Journal of Quantitative Spectroscopy and Radiative Transfer* **147** 145-54
- [19] Tarvainen T, Vauhkonen M, Kolehmainen V and Kaipio J P 2005 Finite element model for the coupled radiative transfer equation and diffusion approximation *International Journal for Numerical Methods in Engineering* **65** 383-405
- [20] McClarren R G and Hauck C D 2010 Simulating radiative transfer with filtered spherical harmonics *Physics Letters A* **374** 2290-6
- [21] Ren K, Bal G and Hielscher A H 2006 Frequency Domain Optical Tomography Based on the Equation of Radiative Transfer *SIAM Journal on Scientific Computing* **28** 1463-89
- [22] Rutily B and Chevallier L 2006 Why is it so difficult to solve the radiative transfer equation? *EAS Publications Series* **18** 1-23
- [23] Zheng H and Han W 2011 On simplified spherical harmonics equations for the radiative transfer equation *Journal of Mathematical Chemistry* **49** 1785-97

- [24] Ren N, Liang J, Qu X, Li J, Lu B and Tian J 2010 GPU-based Monte Carlo simulation for light propagation in complex heterogeneous tissues *Opt. Express* **18** 6811
- [25] Katzgraber H G, Trebst S, Huse D A and Troyer M 2006 Feedback-optimized parallel tempering Monte Carlo *Journal of Statistical Mechanics: Theory and Experiment*
- [26] Xiong W and Dai Y 2012 Dynamical Monte Carlo studies of the three-dimensional bimodal random-field Ising model *Journal of Statistical Mechanics: Theory and Experiment* **2012**
- [27] Fichtorn K A and Weinberg W H 1991 Theoretical foundations of dynamical Monte Carlo simulations *The Journal of Chemical Physics* **95** 1090-6
- [28] Salah M B, Askri F, Rouse D and Ben Nasrallah S 2005 Control volume finite element method for radiation *Journal of Quantitative Spectroscopy and Radiative Transfer* **92** 9-30
- [29] de Oliveira J V P, Cardona A V, Vilhena M T and Barros R C 2002 A semi-analytical numerical method for time-dependent radiative transfer problems in slab geometry with coherent isotropic scattering *Journal of Quantitative Spectroscopy and Radiative Transfer* **73** 55-62
- [30] Frank M, Klar A, Larsen E W and Yasuda S 2007 Time-dependent simplified PN approximation to the equations of radiative transfer *Journal of Computational Physics* **226** 2289-305
- [31] Kasen D, Thomas R C and Nugent P 2006 Time-dependent Monte Carlo Radiative Transfer Calculations for Three-dimensional Supernova Spectra, Light Curves, and Polarization *The Astrophysical Journal* **651** 366-80
- [32] Francoeur M and Rouse D R 2007 Short-pulsed laser transport in absorbing and scattering media: Time-based versus frequency-based approaches *Journal of Physics D: Applied Physics* **40** 5733-42
- [33] Sterpin E, Salvat F, Olivera G H and Vynckier S 2008 Analytical model of the binary multileaf collimator of tomotherapy for Monte Carlo simulations *Journal of Physics: Conference Series* **102**
- [34] Golse F and Perthame B 1986 Generalized solutions of the radiative transfer equations in a singular case *Communications in Mathematical Physics* **106** 211-39
- [35] Liemert A and Kienle A 2013 Exact and efficient solution of the radiative transport equation for the semi-infinite medium *Sci. Rep.* **3**
- [36] Klose A D, Netz U, Beuthan J and Hielscher A H 2002 Optical tomography using the time-independent equation of radiative transfer — Part 1: forward model *Journal of Quantitative Spectroscopy and Radiative Transfer* **72** 691-713
- [37] Koch R and Becker R 2004 Evaluation of quadrature schemes for the discrete ordinates method *Journal of Quantitative Spectroscopy and Radiative Transfer* **84** 423-35